CHAPTER 10

In silico investigation on the effect of Epigallocatechin gallate (EGCG) on the interaction between p53 (NTD) and MDM2 (NTD)

In silico investigation on the effect of Epigallocatechin gallate (EGCG) on the interaction between p53 (NTD) and MDM2 (NTD)

10.1. Abstract:

The protein MDM2 is an important antagonistic regulator of the tumour suppressor p53 molecule. Therefore, to control the activity of the p53 gene, it is important to limit the interaction between MDM2 and p53 molecules. Recently, a small molecule named Epigallocatechin gallate (EGCG) was found to bind to the NTD of p53 molecule, causing the p53 molecules to resume their normal function. In this study, we have studied the interaction profile as well as the structural dynamics of p53(NTD)-EGCG complex using molecular dynamics simulation. It was found that the molecule EGCG remains intact with the TAD1 of p53(NTD) throughout the simulation.. We also carried out the BFE as well as PRED analyses for the p53(NTD)-EGCG complex. The binding affinity was found to be good ($\Delta G_{binding}$ = -9.79 kcal mol^{-1}), and residues GLU28, MET40 and LYS24 of p53 provide the highest energy contributions for the interaction between p53 and EGCG.

10.2. Introduction:

Mutations in the tumor-suppressor protein p53 are present in around 50% of all human cancers [691]. There is a nearly unanimous mutation (96%) in serous ovarian cancer as well as a rare frequency (10%) in thyroid cancer among p53 mutations [692], which are more common in some cancer types than others. It is therapeutically possible to target p53 wild-type (WT) malignancies differently than p53 mutant tumours as a result of this disparity [693]. Numerous preclinical investigations have shown that the restructuring of mutant p53 to its active, usual WT conformation promotes apoptosis and causes tumour regression [694].

Normal conditions result in low intracellular levels of p53 due to the proteasome's quick degradation of p53. Numerous signaling mechanisms, including as sumoylation, methylation, phosphorylation, glycosylation, and acetylation, have the potential to affect its degradation [695, 696]. Both ubiquitin-dependent and ubiquitin-independent ways of

occurrence are possible [697,698]. The most important among them is ubiquitination [699]; and the major inhibitor of p53 [700] is the E3 ligase MDM2; p53 also interacts with a variety of other E3 and E4 ligases. The p53 N-terminal TAD binds with MDM2's N-terminal, promoting p53's C-terminal RING finger E3 ligase activity and enabling ubiquitin to be transported to a number of lysine residues in both the core DNA-binding and C-terminal regulatory domains of p53 [701]. MDM2 ubiquitination severely affects p53's transcriptional activity (mono/poly-ubiquitination). Mono-ubiquitin stimulates nuclear export, while poly-ubiquitin targets nuclear p53 for proteasome degradation. Furthermore, p53 increases MDM2 transcriptionally; this negative feedback loop, together with the cyclical regulation of both proteins, ensures that p53 levels are maintained low under typical conditions [702].

A common beverage enjoyed by people all over the world, green tea has been shown to have inhibitory activity against a number of cancers, including breast, lung, prostate, and colon cancer [704-711]. The majority of green tea's anticancer properties are related to its polyphenol components, the most significant of which is epigallocatechin-3-gallate (EGCG) [712-719]. 50–80% of the catechin in green tea is made up of EGCG [720-727]. p53 was discovered to be crucial in the apoptosis and cell growth arrest caused by EGCG [728-731]. A library of 2295 phytochemicals was used to identify EGCG as an inhibitor of the p53-MDM2 interaction in a recent study [732-734]. It is not yet known how EGCG alters the interaction between MDM2 and p53 at the molecular level in details.

In the present study, we have investigated the conformational dynamics and stability, as well as the interaction profile in details of the p53(NTD)-EGCG complex. We also carried out BFE and PRED analyses to infer the binding characteristics and identify hotspot residues across the interface of MDM2(NTD) in the p53(NTD)-EGCG complex.

10.3. Materials & Methods:

10.3.1. Preparation of the p53(NTD)-EGCG system:

The 3-D structure of p53 NTD, comprising of amino acid residues from 1-61, was modelled using I- TASSER server by submitting the amino acid (1-61 res) sequence. Five models were then obtained. The best structure was then viewed using the UCSF Chimera software v.1.13.1.

The 3-D structure of Epigallocatechin gallate (EGCG) (PubChem CID: 65064), was procured from the PubChem server in SDF file format and then PDB file format for the same was obtained using the open Babel online server. The small molecule EGCG was then visualised using the ArgusLab visualization software v.4.0.1, followed by its energy optimization by the UFF (universal force field).

The PatchDock web server was then used to prepare the p53(NTD)-EGCG complex. The best docked model was chosen based on section based on the principle mentioned in section **7.3.1**.

10.3.2. MD simulation of the p53(NTD)-EGCG complex:

The MD simulation study on the p53(NTD)-EGCG complex was then performed using the Assisted Model Building with Energy Refinement (AMBER) 14 software package, where ff99SB force field parameters were used for the protein part of the system, while the ligand (EGCG) was treated with the generalized AMBER force field (GAFF) parameters. The rest of the steps were performed as mention in section **7.3.2**.

10.3.3. Analysis of the MD Trajectories:

The analysis of the MD trajectories have been performed using the modules mentioned in section **4.3.3**.

10.3.4. LigPlot Analysis of the p53(NTD)-EGCG complex:

Using the RMSD clustering algorithm, the conformer of the complex at the beginning of the simulation (0 ns) and the conformer of the complex at the end of the simulation (50 ns) were extracted from the 50 ns MD trajectories. The confermers were then subjected to Ligplot analysis to obtain the Protein-Ligand interaction profiles.

10.3.5. BFE and PRED Analyses of the p53(NTD)-EGCG complex:

The BFE and the PRED of the p53(NTD)-EGCG complex interface residues analyses

were carried out using the procedure mentioned in section **4.3.6.**

10.3.6. Determination of the interface residues:

Using the RMSD clustering algorithm, p53(NTD)-EGCG complex stucture conformers at the beginning of the simulation (0 ns), as well as at the end of the simulation (50 ns) were extracted. Then EGCG was removed from the both the conformers of the p53(NTD)-EGCG complex. On the other hand the 3-D structure of MDM2 bound to the TAD1 of p53 protein (PDB ID: 1YCR) was obtained from the RCSB PDB [27], followed by the extraction of MDM2(NTD) from the p53-MDM2 complex. Then, the p53(NTD) extracted from the 0 ns connformer was docked with the MDM2(NTD) extracted (System 1), on the other hand, the p53(NTD) extracted from the 50 ns connformer was docked with the MDM2(NTD) extracted (System 2). using ClusPro 2.0 online server. Both the complex structures obtained (System 1 and 2) were then uploaded in the PDBsum server to obtain the Protein-Protein interaction (PPI) profiles.

10.4. Results & Discussions:

10.4.1. Analysis of the conformational changes of the p53(NTD)-EGCG Complex:

We have performed MD simulation on the p53(NTD)-EGCG complex. After equilibration, the complex was subjected to production dynamics for 50 ns (**Figure 10.1**). From **Figure 10.1**, it can be observed that EGCG remains bound to the TAD1 of p53(NTD) throughout the simulation.

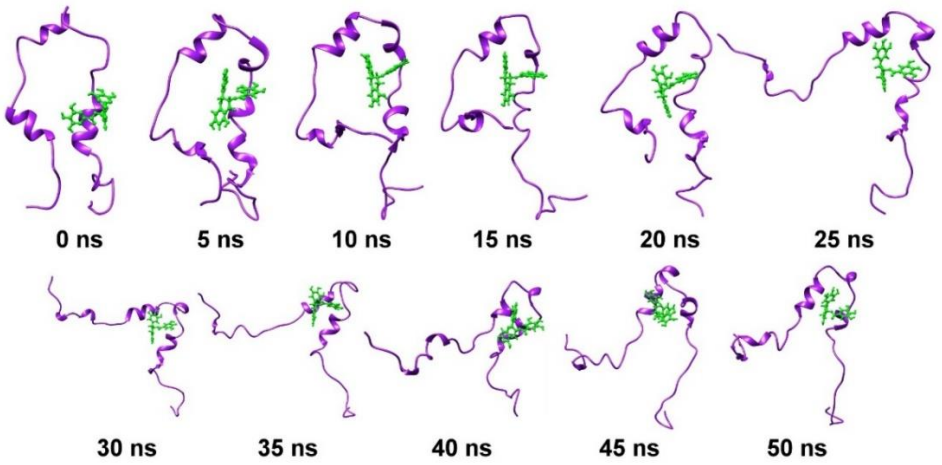

Figure 10.1. *Conformations of p53(NTD)-EGCG at different time intervals of simulation.*

Various structural properties such as RMSD, RMSF, Rg, SASA, number of intermolecular hydrogen bonds, and the secondary structural elements were evaluated separately for p53(NTD)-EGCG complex.

10.4.2. RMSD analysis of the p53(NTD)-EGCG Complex:

The RMSD graph was plotted for Cα atoms for the complex as shown in **Figure 10.2**. We observed RMSD oscillate till 20 ns of simulation time and then found settled for the rest of the simulation time. The average RMSD value of p53(NTD)-EGCG complex was found to be 7 Å.

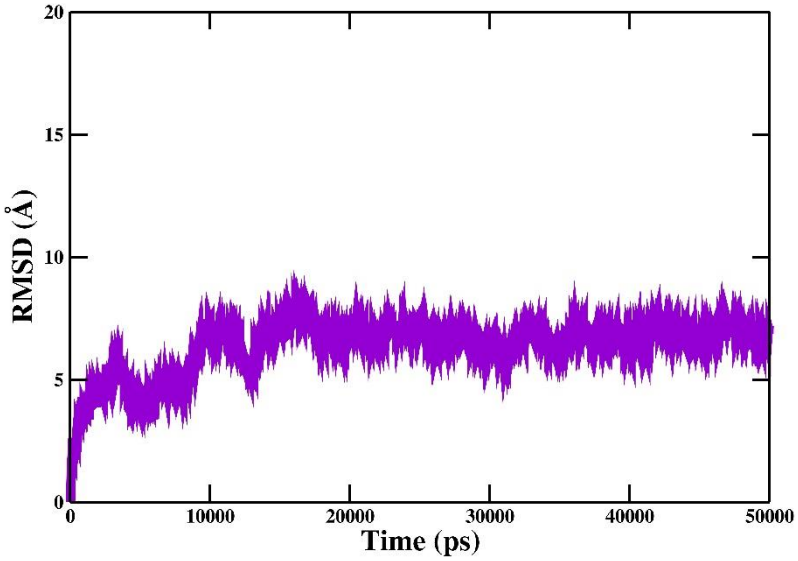

Figure 10.2. *RMSD analysis of p53(NTD)-EGCG complex.*

10.4.3. RMSF analysis of the p53(NTD)-EGCG Complex:

Then we determined the Residue flexibility in the p53(NTD)-EGCG complex using RMSF analysis. **Figure 10.3.** shows the RMSF values for C-α atoms of the complex. From the RMSF plot, we see fluctuation of C-α atoms only in the N-Terminal and C-Terminal residues of p53(NTD).

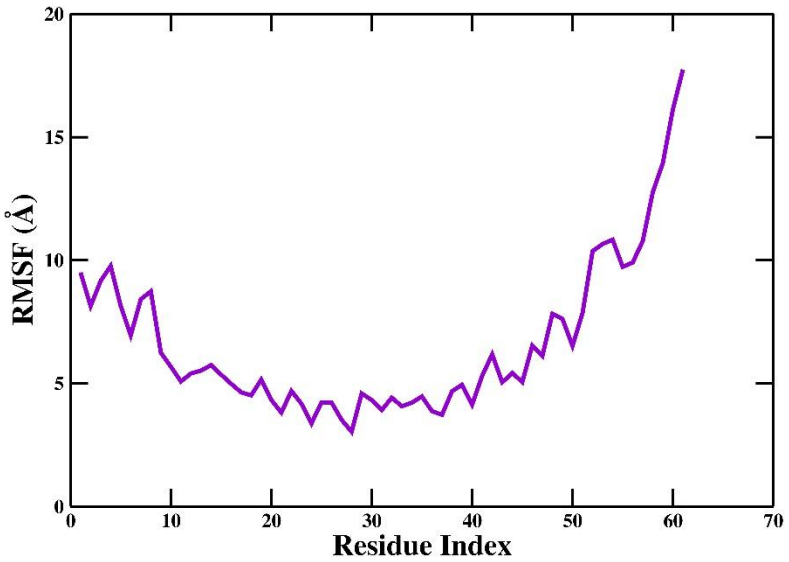

Figure 10.3. *RMSF analysis of p53(NTD)-EGCG complex.*

10.4.4. Rg analysis of the p53(NTD)-EGCG Complex:

Rg is another important geometrical parameter, which indicates the compactness of a system over a period of simulation time. A protein molecule must maintain its compactness at the right temperature and pressure to be considered stable. The average Rg values for the p53(NTD)-EGCG complex was found to be 16 Å, which remained constant throughout the simulation (**Figure 10.4**).

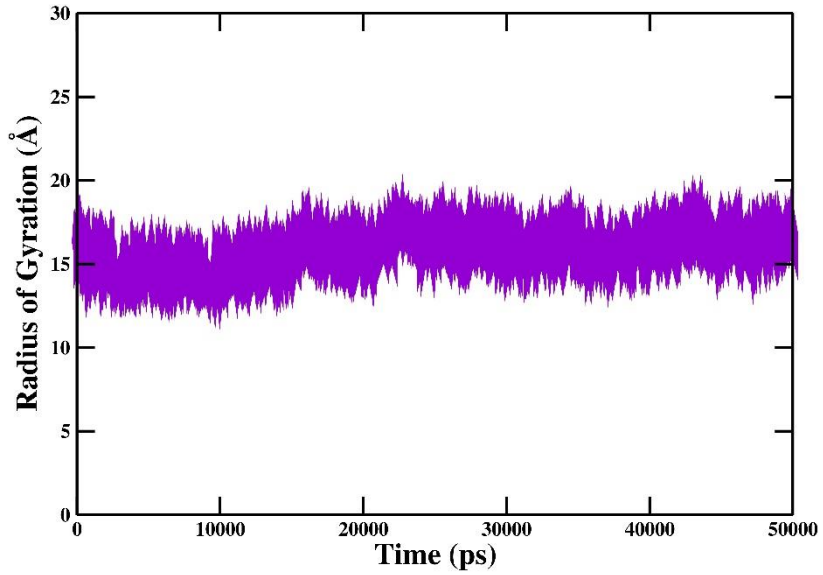

Figure 10.4. *Rg analysis of p53(NTD)-EGCG complex.*

10.4.5. SASA analysis of the p53(NTD)-EGCG Complex:

The SASA gives an overview of the behavior of residues with respect to solvent, and determines the stability of the protein. The SASA for p53(NTD)-EGCG complex was calculated to be 6500 $Å^2$ (**Figure 10.5**).

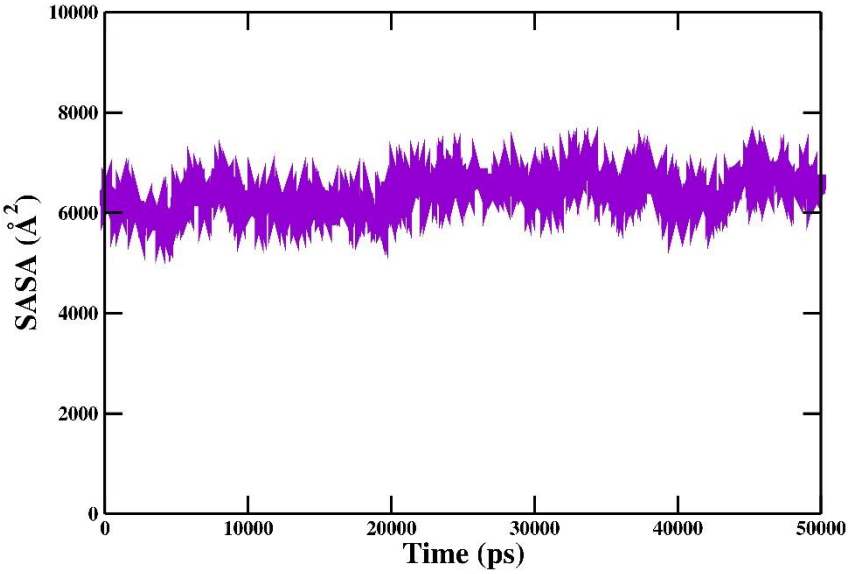

Figure 10.5. *SASA analysis of p53(NTD)-EGCG complex.*

10.4.6. Hydrogen bond analysis of the p53(NTD)-EGCG Complex:

Additionally, we also carried out the analysis of inter-molecular hydrogen bonds present in the p53(NTD)-EGCG complex. The number of hydrogen bonds was observed to be

within the ideal range as proposed for the globular proteins. **Figure 10.6** represents the intermolecular hydrogen bond analysis of the complex. The average number of intermolecular hydrogen bonds in the complex with p53(NTD) as donor and EGCG as acceptor was found to be 2, and with EGCG as donor and p53(NTD) as acceptor was found to be 4.

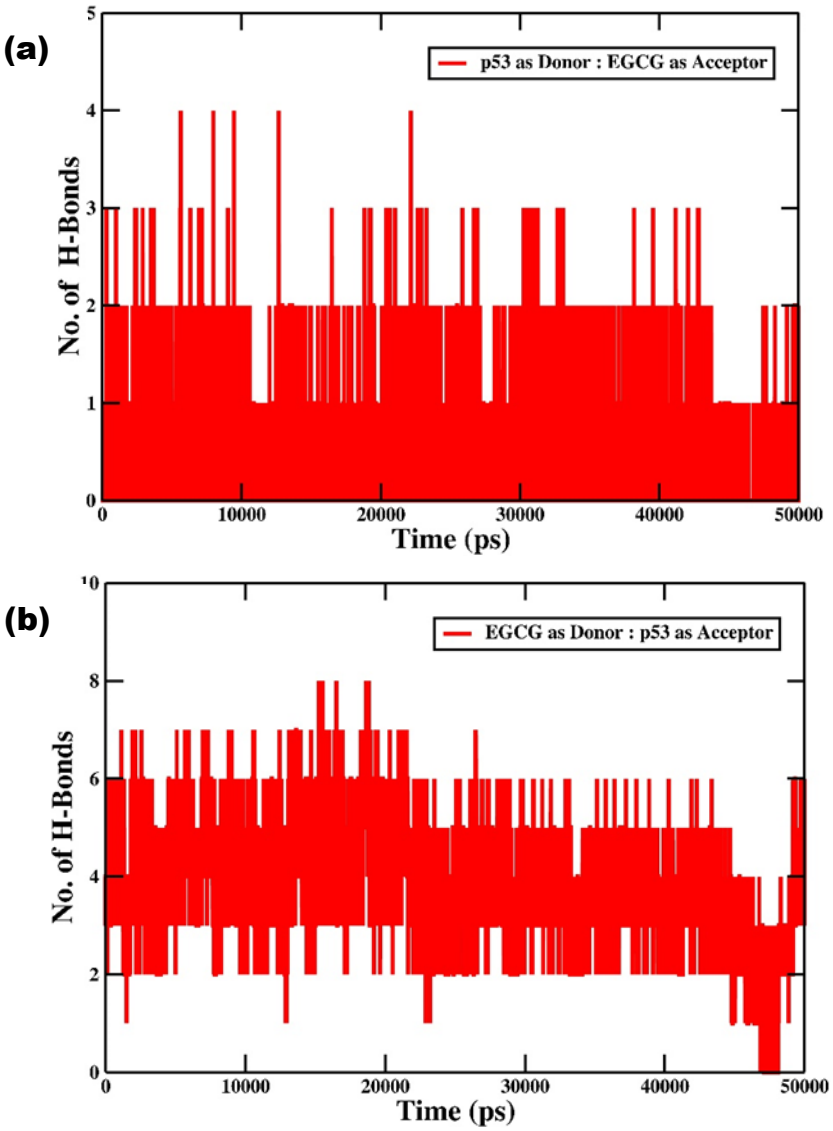

Figure 10.6. *Inter-molecular hydrogen bond analysis of p53(NTD)-EGCG complex with (a) p53 as Donor and EGCG as acceptor; and (b) EGCG as Donor and p53 as acceptor.*

10.4.7. Analysis of probable secondary structure per residue of p53(NTD) in the p53(NTD)-EGCG Complex:

Then we carried out the analysis of the probable secondary structure that each residue of p53(NTD) can adopt in p53(NTD)-EGCG complex (**Figure 10.7**). From **Figure 10.7,**

we infer that the p53(NTD) molecule contains the secondary structure α-helix predominantly in the regions 18-53 residues.

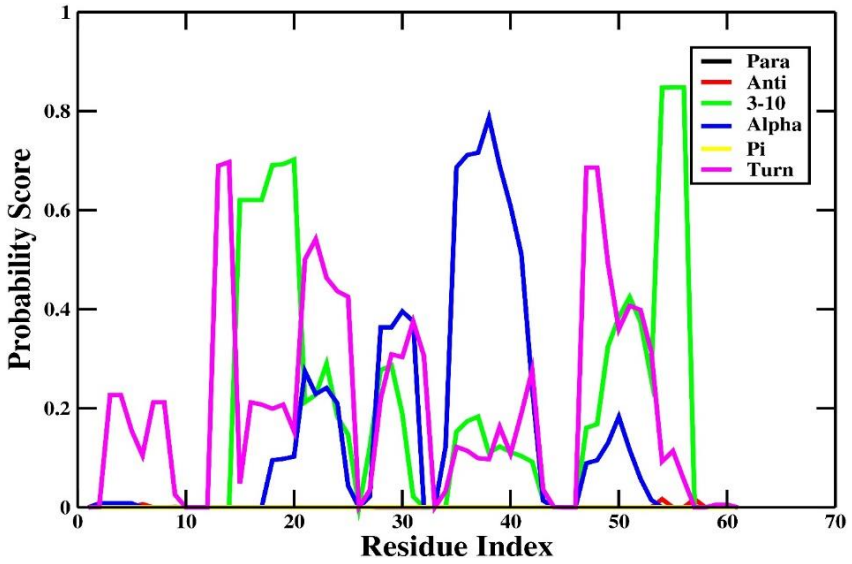

Figure 10.7. *Probability score for secondary structure analysis of p53(NTD) in the p53(NTD)-EGCG complex.*

10.4.8. DSSP analysis of p53(NTD) in the p53(NTD)-EGCG Complex:

Then we performed the DSSP analysis using the Kabsch and Sander algorithm to study the changes in secondary structural elements in the p53(NTD) molecule (as shown in **Figure 10.8**). From **Figure 10.8**, it can be observed that there is an increase in the $\alpha/3_{10}$-helix content during the simulation, resulting in a good binding affinity between p53(NTD) and EGCG.

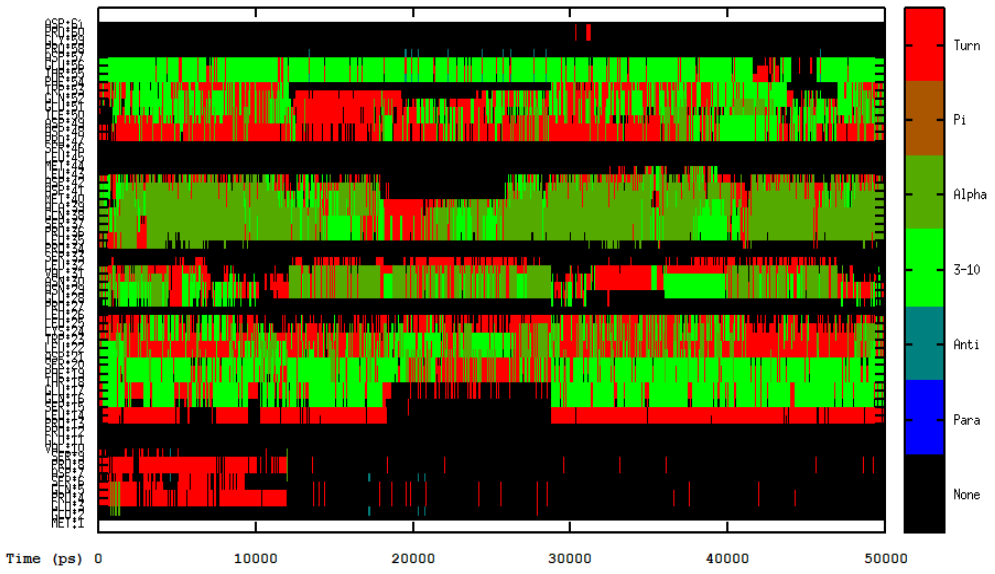

Figure 10.8. *The evolution of secondary structure evaluated using DSSP is shown for MDM2 molecule in p53(NTD)-EGCG complex.*

10.4.9. Secondary Structure analysis of the conformers of the p53(NTD)-EGCG Complex:

In addition, the secondary structure content of p53(NTD) present in the p53(NTD)-EGCG complex at the beginning of the simulation (0 ns), as well as at the end of the simulation (50 ns) have been calculated using the 2StrucCompare server (**Table 10.1**), by extracting the conformers using RMSD clustering algorithm, and then uploading them in the online server. It was found that p53(NTD) in the p53(NTD)-EGCG complex at 0 ns has 24.6% helices, while p53(NTD) in the p53(NTD)-EGCG complex at 50 ns has 34.4% helices.

Table 10.1. *Secondary structure analysis of the initial and final structures of p53-EGCG complex using 2Struc online server.*

p53(NTD)-EGCG	***α-Helix (%)***	***3_{10}-Helix (%)***	***Turns (%)***
0 ns	*18.0*	*6.6*	*37.7*
50 ns	*23.0*	*11.5*	*13.1*

10.4.10. BFE and PRED analyses of the p53(NTD)-EGCG Complex:

The BFE calculations of p53(NTD) and EGCG to form the p53(NTD)-EGCG complex were performed using the MM-GBSA method, a module of the AMBER14 software package. The BFE evaluated for the p53(NTD)-EGCG complex, together with the descriptions of the energy terms, are shown in Table **10.2**. From Table **10.2**, all the derived components required for the BFE analysis have been observed to contribute to the binding of p53(NTD) and EGCG to form the p53(NTD)-EGCG complex. The total BFE ($\Delta G_{binding}$) was found to be -9.79 kcal mol $^{-1}$, which indicates a good binding affinity between p53(NTD) and EGCG molecule in the p53(NTD)-EGCG complex.

Table 10.2. *The various components of the BFE (kcal mol^{-1}) evaluated by MM/GBSA method between p53(NTD)-EGCG complex.*

Components	Complex (kcal mol^{-1})	Standard Deviation (±)	Receptor (kcal mol^{-1})	Standard Deviation (±)	Ligand (kcal mol^{-1})	Standard Deviation (±)	$\Delta\Delta G_{bind}$ (kcal mol^{-1})	Standard Deviation (±)
$\Delta E_{VDWAALS}$	-326.94	9.07	-292.49	7.31	-6.20	0.63	-28.25	4.72
ΔE_{EL}	-3015.02	29.05	-2829.74	28.44	-108.62	4.76	-76.67	8.01
ΔE_{GB}	-2983.88	22.89	-2991.10	23.07	-74.07	2.88	81.29	4.89
ΔE_{SURF}	47.12	0.53	47.65	0.53	4.01	0.04	-4.54	0.20
ΔG_{gas}	1693.22	33.24	1811.50	31.44	-13.37	6.38	-104.91	5.66
ΔG_{solv}	-2936.76	22.94	-2943.45	23.10	-70.05	2.87	76.75	4.91
ΔG_{TOTAL}	-1243.54	23.13	-1131.95	21.84	-83.42	5.31	**-28.16**	2.30
TS_{TRA}	15.65	0	15.59	0	13.20	0	-13.13	0
TS_{ROT}	15.99	0.04	15.94	0.09	11.12	0	-11.07	0.10
TS_{VIB}	764.87	2.68	725.21	3.97	33.82	0.06	5.83	4.88
TS_{TOTAL}	796.51	2.71	756.74	4.02	58.13	0.06	**-18.37**	4.94
$\Delta G_{binding}$							**-9.79**	

ΔE_{EL} = electrostatic energy as calculated by the MM force field; $\Delta E_{VDWAALS}$ = van der Waals contribution from MM; ΔE_{GB} = the electrostatic contribution to the polar solvation free energy calculated by GB; ΔE_{SURF} = non-polar contribution to the solvation free energy calculated by an empirical model; ΔG_{gas} = total gas phase energy ($\Delta G_{gas} = \Delta E_{EL} + \Delta E_{VDWAALS}$);$\Delta G_{solv}$ = sum of nonpolar and polar contributions to solvation; ΔG_{TOTAL} = final estimated binding free energy in kcal mol^{-1} calculated from the terms above ($\Delta G_{TOTAL} = \Delta G_{gas} + \Delta G_{solv}$); TS_{TRA} = translational energy; TS_{ROT} = rotational energy; TS_{VIB} = vibrational energy; TS_{TOTAL} = total entropic contribution; and $\Delta G_{binding}$ = BFE.

To have an insight into the influence of each of the amino acid residues of p53(NTD) on the overall p53(NTD)-EGCG interaction, PRED values were determined implying the MM-GBSA method. **Figure 10.9** represents the PRED analysis for the interface residues of p53(NTD) present in the p53(NTD)-EGCG complex. The highest energy contribution can be observed from the residue GLU28, followed by residues MET40 and LYS24 of p53(NTD) respectively.

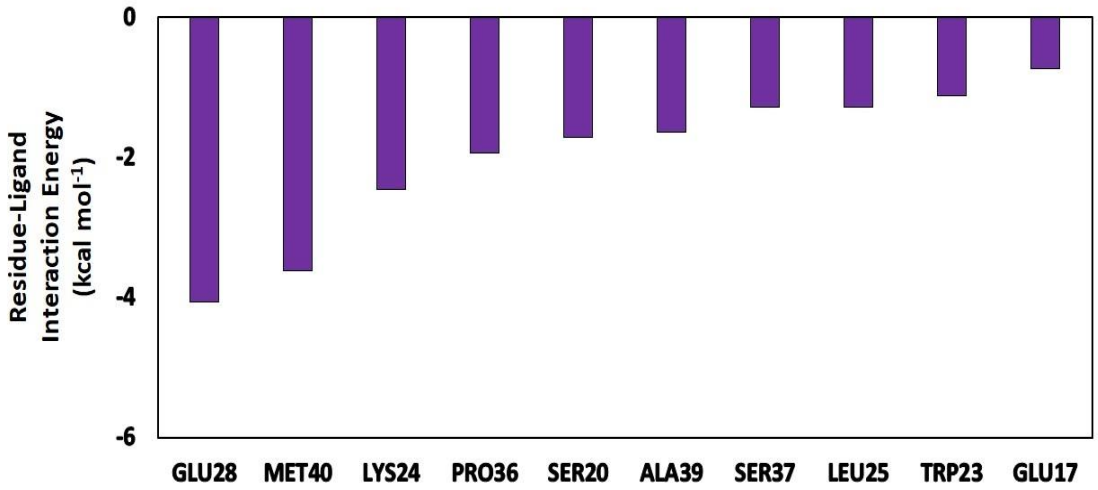

Figure 10.9. *Per Residue Energy Decomposition (PRED) analysis of p53(NTD) in p53(NTD)-EGCG complex.*

10.4.11. LigPlot analysis of the conformers of the p53(NTD)-EGCG Complex:

The structures of the complex extracted at the beginning of MD simulation (0 ns) and at the end of the simulation (50 ns) were then subjected to LigPlot analysis to obtain the protein-ligand interaction profiles (**Figure 10.10**). Only two hydrogen bonds can be observed in the p53(NTD)-EGCG complex at the beginning of the MD simulation. Whereas, five hydrogen bonds can be observed in the p53-EGCG complex at the end of the MD simulation.

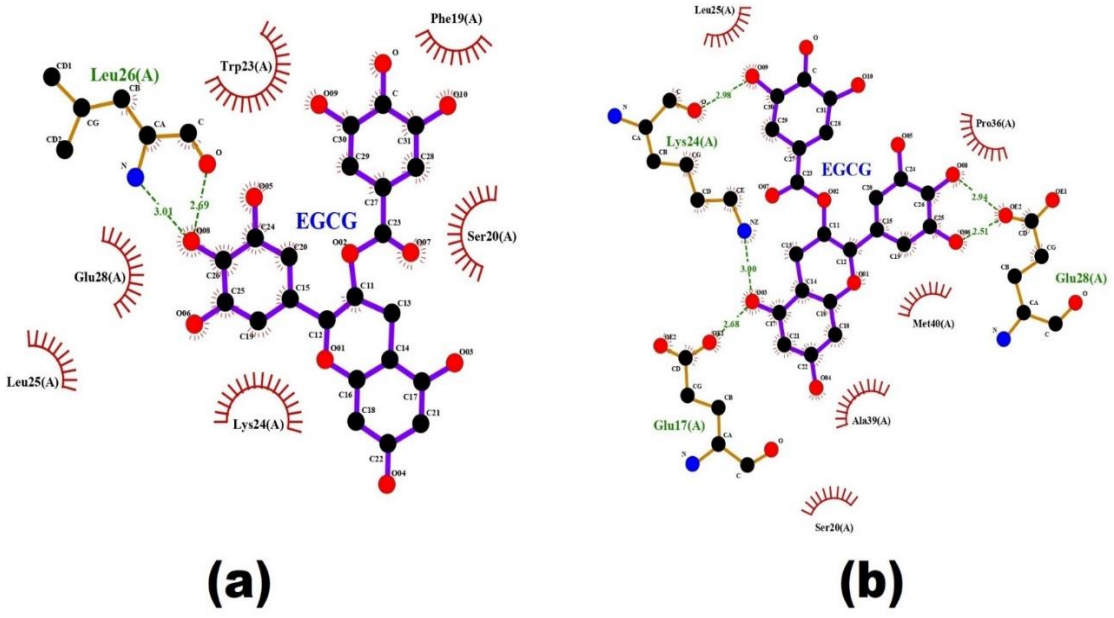

Figure 10.10. *Protein-Ligand Interaction Profile of p53-EGCG complex at (a) the beginning of MD simulation, and (b) the end of MD simulation.*

10.4.12. Determination of the interface residues of the conformers of the p53(NTD)-EGCG Complex:

Then, the two systems mentioned earlier: Sytem 1 and 2 were visualised using UCSF Chimera software v.1.13.1. It can be observed that the TAD1 present in p53(NTD) fits into the binding cavity of MDM2(NTD) before MD simulation of p53(NTD)-EGCG complex (**Figure 10.11a**). Whereas, the TAD1 present in p53(NTD) does not fit into the binding cavity of MDM2(NTD) at the end of MD simulation of p53(NTD)-EGCG complex (**Figure 10.11b**). This indicates that the p53(NTD), in complex with EGCG, undergoes conformational changes throughout the simulation, resulting in the disruption of p53(TAD1)-MDM2(NTD) interaction.

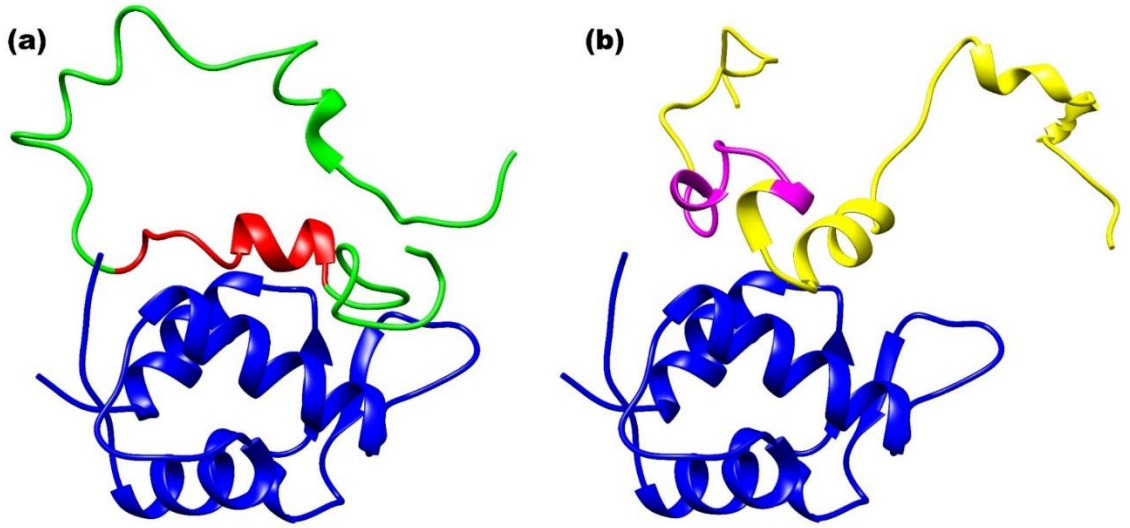

Figure 10.11. *MDM2(NTD) docked with p53(NTD) extracted from the p53-EGCG complex (a) before the MD simulation of the p53-EGCG complex, and (b) at the end of the MD simulation of the p53-EGCG complex. Blue=MDM2(NTD), Green=p53(NTD) before simulation, Red=p53(TAD1) before simulation, Yellow=p53(NTD) after simulation, Purple=p53(TAD1) after simulation.*

After obtaining the protein-protein interaction profiles of the two systems, they were compared with the protein-protein interaction profile of p53(TAD1)-MDM2(NTD), which is already present in the PDBsum Database (System 3). It can be observed that the number of residues from p53(NTD) interacting with MDM2(NTD) before simulation are more in common with p53(NTD) interacting with MDM2(NTD) in system 3 than the number of residues from p53(NTD) interacting with MDM2(NTD) at the end of simulation common with p53(NTD) interacting with MDM2(NTD) in system 3. Also, the total number of residues from MDM2(NTD) interacting p53(NTD) in system 1 is

more than the total number of residues from MDM2(NTD) interacting p53(NTD) in system 2 (**Figure 10.12**).

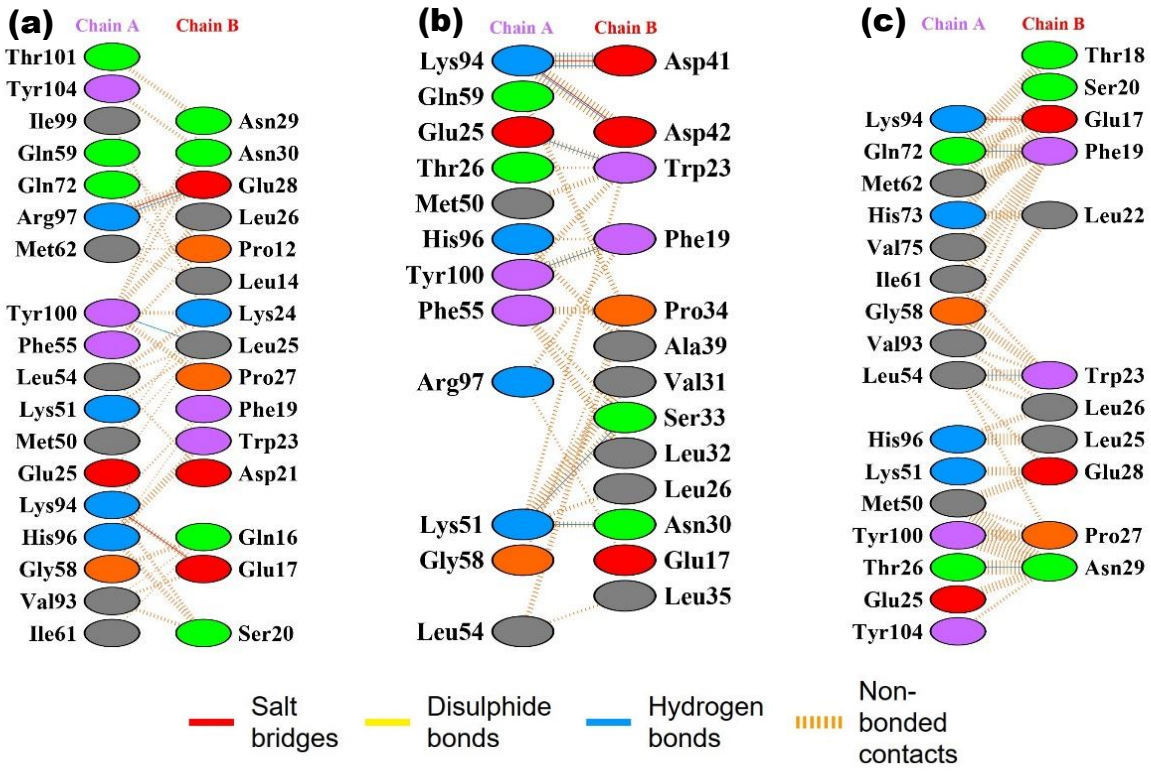

Figure 10.12. *Protein-Protein Interaction Profile of (a) MDM2(NTD)-p53(NTD) complex before p53-EGCG simulation, (b) MDM2(NTD)-p53(NTD) complex after p53-EGCG simulation, and (c) MDM2-p53 complex (PDB ID: 1YCR). Chain A: MDM2, Chain B: p53.*

10.5. Conclusion:

In this study, we have investigated the molecular interactions and structural dynamics in details between p53 and its inhibitor EGCG. The small molecule EGCG remains bound to the TAD1 of p53(NTD) throughout the simulation. The percentage of alpha-helices increase throughout the simulation, resulting in a good binding affinity between EGCG and p53(NTD). There exists a good binding affinity between the p53(NTD) and EGCG was ($\Delta G_{binding}$ = -9.79 kcal mol^{-1}). The residues GLU28, MET40 and LYS24 of p53(NTD) provide the highest energy contributions for the interaction between p53(NTD) and EGCG. The results of our investigation may be used to create more potent p53-MDM2 interaction inhibitors, enhancing the efficacy of cancer treatment.